01 Jan 2013

Universal Emergence of Spatially Modulated Structures Induced by Flexoantiferrodistortive Coupling in Multiferroics

Eugene A. Eliseev

Sergei V. Kalinin

Yijia Gu
Missouri University of Science and Technology, guyij@mst.edu

Maya D. Glinchuk

et. al. For a complete list of authors, see https://scholarsmine.mst.edu/matsci_eng_facwork/2490

Recommended Citation

E. A. Eliseev et al., "Universal Emergence of Spatially Modulated Structures Induced by Flexoantiferrodistortive Coupling in Multiferroics," *Physical Review B - Condensed Matter and Materials Physics*, vol. 88, no. 22, American Physical Society (APS), Jan 2013.
The definitive version is available at https://doi.org/10.1103/PhysRevB.88.224105

Universal emergence of spatially modulated structures induced by flexoantiferrodistortive coupling in multiferroics

Eugene A. Eliseev,[1] Sergei V. Kalinin,[2,*] Yijia Gu,[3] Maya D. Glinchuk,[1] Victoria Khist,[1] Albina Borisevich,[2] Venkatraman Gopalan,[3] Long-Qing Chen,[3] and Anna N. Morozovska[4,†]

[1]*Institute for Problems of Materials Science, National Academy of Sciences of Ukraine, 3, Krjijanovskogo, 03142 Kiev, Ukraine*

[2]*The Center for Nanophase Materials Sciences, Oak Ridge National Laboratory, Oak Ridge, Tennessee 37831, USA*

[3]*Department of Materials Science and Engineering, Pennsylvania State University, University Park, Pennsylvania 16802, USA*

[4]*Institute of Physics, National Academy of Sciences of Ukraine, 41, prospekt Nauki, 03028 Kiev, Ukraine*

(Received 21 January 2013; published 19 December 2013)

We proved the existence of a universal flexoantiferrodistortive coupling as a necessary complement to the well-known flexoelectric coupling. The coupling is universal for all antiferrodistortive systems and can lead to the formation of incommensurate, spatially modulated phases in multiferroics. Our analysis can provide a self-consistent mesoscopic explanation for a broad range of modulated domain structures observed experimentally in multiferroics.

DOI: 10.1103/PhysRevB.88.224105 PACS number(s): 77.80.Jk, 75.85.+t, 77.80.bg, 77.80.bn

I. INTRODUCTION

Multiferroics, materials with multiple coupled order parameters, have emerged as an important topic in condensed matter physics[1,2] due to both their intriguing physical behaviors and a broad variety of novel physical applications they enable. The unique physical properties of multiferroics originated from the complex interactions among the structural, polar, and magnetic long-range order parameters.[3,4] For instance, biquadratic and linear magnetoelectric couplings lead to intriguing effects such as giant magnetoelectric tunability of multiferroics.[5,6] Biquadratic coupling of the structural and polar order parameters, introduced by Haun,[7] Salje *et al.*,[8] Balashova and Tagantsev,[9] and Tagantsev *et al.*,[10] are responsible for the unusual behavior of the dielectric and polar properties in ferroelastics–quantum paraelectrics. Daraktchiev *et al.*[11] considered the influence of biquadratic coupling between polarization and magnetization on the structure of ferroelectric domain walls in multiferroics. Dieguez *et al.*[12] found that the behavior of the structural order parameter at the domain walls of multiferroic $BiFeO_3$ determines their structure and energy. In this regard, new intriguing phenomena emerging in nanoscale phase-separated ferroics can be represented as extremely dense domain structures.

Nanoscale phase separation in materials ranging from giant magnetoresistive manganites,[13–15] ferroelectric relaxors,[16,17] and morphotropic materials,[18–20] martensites,[21,22] and birelaxors[23] remains one of the active topics of research in condensed matter physics. Experiment[24] revealed the existence of the incommensurate modulation at the structural domain boundaries in multiferroic $Bi_ySm_{1-y}FeO_3$. Antiferrodistortive[25] and superstructural dynamic antiferroelectric-antiferrodistortive[26] modulation have also recently been observed in multiferroic $EuTiO_3$.

There are also a wide variety of modulated domain structures observed experimentally at the morphotropic boundaries in multiferroics, which are usually identified as monoclinic phase regions by scattering. They offer rich evidence for spatially modulated structures in electron microscopy.[27–30] In particular the apparent "orthorhombic" phase in PMN-$PbTiO_3$ exists as an adaptive tetragonal phase.[27] Domains with low domain-wall energy corresponding to monoclinic ferroelectric states[28] and pseudo-monoclinic phase[29] were revealed near the morphotropic phase boundaries in $Pb_xZr_{1-x}TiO_3$. Also it is worth mentioning the adaptive phases in shape-memory martensite alloys, which are, in fact, adaptive modulations.[30]

A. Flexoelectric effects

To get insight into the physical properties of domain walls and interfaces in multiferroics at the meso- and nanoscale, deep understanding of *flexo-type couplings* between the gradients of the polar and other order parameters is extremely important. The coupling between the polarization gradient components $\partial P_k/\partial x_l$ and other order parameters' contribution to the thermodynamic potential is

$$\delta U = K_{ijkl} w_{ij} \frac{\partial P_k}{\partial x_l}, \tag{1}$$

where K_{ijkl} is the corresponding "flexo-type" tensor. Relationships between the dyadic tensor w_{ij} and the order parameters are listed in Table I.

In its initial form the flexoelectric coupling between the polarization and strain gradient is universal for macro- and nanoscale objects.[41–45] Flexoelectric and all other couplings from Table I lead to the appearance of improper ferroelectricity in multiferroics with the inhomogeneous spontaneous strain,[32] magnetization,[33,34] aniferromagnetic,[35,36] or antiferroelectric order parameter[24] or antiferrodistortions. Here, we explore the antiferrodistortive coupling, since antiferrodistortive modes are virtually present in all the perovskites. Besides the fact that the flexoantiferrodistortive coupling can be of purely fundamental interest, we will demonstrate that it can be a source of *incommensurate modulation in multiferroics*.

B. Incommensurate phases (ICPs) in multiferroics

ICP itself as well as the mechanisms of commensurate-incommensurate phase transitions are some of the most intriguing features of multiferroics.[46,47] Two well-established mean-field Landau-type approaches of ICP description exist. The first one considers a one-component long-range order parameter assuming that its gradient coupling coefficient in

TABLE I. Flexotype coupling in multiferroics allowed by symmetry.

Coupling title	Tensor w_{ij}	Description	Reference
Flexoelectric	u_{ij}	u_{ij}: the strain tensor	31,32
Flexomagnetoelectric	$M_i M_j$	M_i: spontaneous magnetization	33,34
Flexoantimagnetoelectric	$L_i L_j$	L_i: antiferromagnetic order parameter (e.g., the difference of sublattices magnetization)	35–37
Flexoferroelectric	$P_i P_j$	P_i: spontaneous polarization	39
Flexoantiferroelectric	$A_i A_j$	A_i: antiferroelectric order parameter (e.g., the difference of sublattices polarization)	24
Flexoantiferrodistortive	$\Phi_i \Phi_j$	Φ_i: antiferrodistortive order parameter [e.g., axial vector of oxygen octahedral rotational modes (Ref. 40)]	This work

the Landau-Ginzburg-Devonshire (LGD) power expansion is negative, and positively defined higher order derivatives cause the ICP.[48–50] The second approach, that seems more relevant to the ICP in multiferroics description, considers at least a two-component order parameter with positive gradient coefficients, conventional LGD functional for each component, and biquadratic coupling between the order parameters and Lifshitz invariant.[38,47,51,52]

In the paper we show that the increase of the flexoantiferrodistortive coupling strength firstly leads to commensurate-incommensurate phase transitions, and then to the antiferroelectriclike phase appearance in multiferroics. The scenario seems principally different from the known couplings[47–52] and is in agreement with experiments.[24–26]

II. UNIVERSAL FLEXOANTIFERRODISTORTIVE COUPLINGS

The linear-quadratic coupling between the long-range order parameters, antiferrodistortive octahedral rotations Φ_i, and polarization P_i gradient, allowed by any symmetry, and thus *universal for all antiferrodistortive materials with spatially inhomogeneities*, has the form of nonlinear Lifshitz invariant:

$$U_{P\Phi}[\mathbf{P},\mathbf{\Phi}] = \frac{\xi^{u,\sigma}_{ijkl}}{2}\left[\Phi_i\Phi_j\frac{\partial P_k}{\partial x_l} - P_k\frac{\partial(\Phi_i\Phi_j)}{\partial x_l}\right]. \qquad (2a)$$

As universal, the flexoantiferrodistortive coupling (2a) must be included in the LGD thermodynamic potentials. Below we will regard Helmholtz free energy as Φ-P-u representation and Gibbs potential as Φ-P-σ representation (u stands for the strain and σ for the stress).

Nonzero components of the coupling tensor $\xi^{u,\sigma}_{ijkl}$ can be readily determined from the symmetry theory; e.g., for the $m3m$ parent phase of most perovskites they are $\xi_{1111} = \xi_{2222} = \xi_{3333}$, $\xi_{1122} = \xi_{1133} = \xi_{3322}$, $\xi_{1212} = \xi_{1313} = \xi_{2323}$. Numerical values of $\xi^{u,\sigma}_{ijkl}$ can be calculated from the first principles or measured experimentally.

The relationship $\xi^{u}_{ijkl} = \xi^{\sigma}_{ijkl} + f_{ijmn}R_{mnkl}$ is valid, where R_{mnkl} is the rotostriction strain tensor and f_{ijmn} is the flexoelectric stress tensor (see Appendix S1 in Supplemental Material[53]). Physical origin of the "renormalization" term $f_{ijmn}R_{mnkl}$ is the joint action of the "indirect" flexoelectric and rotostriction coupling, since the rotostriction causes the spontaneous strain with components $u^{S}_{mn} = R_{mnpq}\Phi_p\Phi_q$.[54] The relationship $\xi^{u}_{ijkl} = \xi^{\sigma}_{ijkl} + f_{ijmn}R_{mnkl}$ explains that the direct coupling (2a) cannot be treated as the simple renormalization of the flexo-roto effect described by the term $f_{ijmn}R_{mnkl}$. However, similar to the flexo-roto coupling,[54] the gradient coupling induces the polarization variation $P_i(\mathbf{r}) \propto \xi^{u,\sigma}_{ijkl}\partial(\Phi_j\Phi_k)/\partial x_l$ in regions where the tilt is spatially inhomogeneous (domains walls, surfaces, interfaces).

The bilinear antiferroelectric-antiferrodistortive coupling term between the polarization gradient and tilt components product, is allowed by *any symmetry* of parent phase in ABO_3 compounds with an antiferrodistortive mode:

$$U_{A\Phi}[\mathbf{A},\mathbf{\Phi}] = \frac{\zeta_{ijk}}{2}\left(A_i\frac{\partial\Phi_k}{\partial x_j} - \Phi_k\frac{\partial A_i}{\partial x_j}\right). \qquad (2b)$$

Coupling *pseudotensor* ζ_{ijk} nonzero components allowed by the material parent phase symmetry can be determined from the symmetry theory for all point groups. Coupling (2b) is invariant in Φ-P-u and Φ-P-σ representations. Numerical value of the nonzero components ζ_{ijk} can be defined either from experiment or from the first principle calculations. Polar (or true) vector $\mathbf{A}$ is the "antipolarization," defined as the difference of polarization in the neighboring equivalent cells a and b, $\mathbf{A} = (\mathbf{P}_a - \mathbf{P}_b)/2$, and axial (or pseudo-) vector $\mathbf{\Phi} = (\mathbf{\Phi}_a - \mathbf{\Phi}_b)/2$ is the structural order parameter, corresponding to the antiferrodistortive rotational modes of oxygen octahedral,[40] $\mathbf{\Phi}_a = -\mathbf{\Phi}_b$, considered hereinafter. The oxygen octahedra are regarded rigidly connected within the layers, so they can only rotate as a whole and distortive (Jahn-Teller) modes will be neglected. Transformation laws of pseudotensor $\zeta^{u,\sigma}_{ijk}$, true vector $\mathbf{A}$, pseudovector $\mathbf{\Phi}$, and coordinate derivative $\partial/\partial x_l$ are $\tilde{\zeta}_{ijk} = \det(B)B_{im}B_{jg}B_{ks}\zeta_{mgs}$, $\tilde{A}_i = B_{ip}A_p$, $\tilde{\Phi}_k = \det(B)B_{kf}\Phi_f$. Here the summation is performed over the repeating indices. $\mathbf{B}$ is the unitary transformation matrix with components B_{ij} $(i,j = 1,2,3)$ representing all the elements of the parent phase point symmetry group. For the case where the transformation laws become identity we do not use the "tilda" symbol, e.g., $\zeta_{ijk} = \det(B)B_{im}B_{jg}B_{ks}\zeta_{mgs}$. The elementary derivation listed in Appendix S1 of Ref. 53 proves that the expression (2b) is indeed invariant with respect to the transformation of the parent phase point symmetry group and with respect to the permutation operation $a \leftrightarrow b$, when $\mathbf{A} \leftrightarrow -\mathbf{A}$ simultaneously with $\mathbf{\Phi} \leftrightarrow -\mathbf{\Phi}$. For the case of cubic symmetry group $m3m$ we calculated that $\zeta^{u,\sigma}_{ijk} \equiv \chi e_{ijk}$, where symbol e_{ijk} is the antisymmetric

TABLE II. Symmetry of the bilinear coupling in typical antiferrodistortive perovskites.

Point group symmetry	Tensor symbol, structure, and/or nontrivial components	
and ABO_3 example	ζ_{ijk} in Eq. (2a)	ξ_{ijkl} in Eq. (2b)
$m3m$ Parent phase of most perovskites	$\zeta_{123} = -\zeta_{213} = \zeta_{231} = -\zeta_{132} = \zeta_{312} = -\zeta_{321}$ $\zeta_{ijk} \equiv \chi e_{ijk}$, χ is a scalar	$\xi_{1111} = \xi_{2222} = \xi_{3333}$, $\xi_{1122} = \xi_{1133} = \xi_{3322}$, $\xi_{1212} = \xi_{1313} = \xi_{2323}$
$4mm$ $(Pb,Zr)TiO_3$	$\zeta_{123} = -\zeta_{213}$, $\zeta_{312} = -\zeta_{321}$, $\zeta_{132} = -\zeta_{231}$	ξ_{1111}, ξ_{1122}, ξ_{1212}, ξ_{1133}, ξ_{3311}, ξ_{1313}, ξ_{1331}, ξ_{3333}
$4/mmm$ $(Sr,Eu)TiO_3$	$\zeta_{123} = -\zeta_{213}$, $\zeta_{312} = -\zeta_{321}$, $\zeta_{132} = -\zeta_{231}$	The same as for $4mm$
mmm $CaTiO_3$	ζ_{123}, ζ_{132}, ζ_{312}, ζ_{213}, ζ_{231}, ζ_{321} (all are different)	ξ_{1111}, ξ_{1122}, ξ_{2211}, ξ_{2222}, ξ_{1212}, ξ_{1221}, ξ_{2233}, ξ_{1133}, ξ_{3311}, ξ_{1313}, ξ_{1331}, ξ_{2323}, ξ_{2332}, ξ_{3333}
$mm2$ $CaTiO_3$	ζ_{123}, ζ_{132}, ζ_{312}, ζ_{213}, ζ_{231}, ζ_{321} (all are different)	The same as for mmm
$3m$ $BiFeO_3$	$\zeta_{112} = \zeta_{121} = \zeta_{211} = -\zeta_{222}$, $\zeta_{123} = -\zeta_{213}$, $\zeta_{312} = -\zeta_{321}$, $\zeta_{132} = -\zeta_{231}$	ξ_{1111}, ξ_{1122}, ξ_{1133}, ξ_{1313}, ξ_{1331}, ξ_{3311}, ξ_{3333}, ξ_{1113}, ξ_{1131}, ξ_{1311}

Levi-Chivita pseudotensor and constant χ is a true scalar (in particular nonzero components are $\zeta^{u,\sigma}_{123} = -\zeta^{u,\sigma}_{213} = \zeta^{u,\sigma}_{231} = \cdots \equiv \chi$ since $e_{123} = -e_{213} = e_{231} = \cdots = 1$). Using the definition of curl operation, for the $m3m$ parent phase Eq. (2b) acquires the form $U_{A\Phi}[\mathbf{A},\mathbf{\Phi}] = \frac{\chi}{2}(\mathbf{A} \cdot \mathrm{rot}\mathbf{\Phi} - \mathbf{\Phi} \cdot \mathrm{rot}\mathbf{A})$.

Due to the universality, the flexoantiferrodistortive coupling (2) can be a significant driving force for the spontaneous onset of spatial modulation in a wide class of partially clamped multiferroics with antiferrodistortive structural order parameter, such as thin films, twin walls, and antiphase boundaries in $Eu_xSr_yBa_{1-x-y}TiO_3$, $Bi_ySm_{1-y}FeO_3$, $Sr_yCa_{1-y}TiO_3$, $Sr_yMn_{1-y}TiO_3$, etc.

The large difference between the coupling (2a) and (2b) is in the different tilt powers of the bilinear coupling tensors ζ_{ijk} and ξ_{ijkl} in typical antiferrodistortive perovskites with $m3m$ parent phase [such as $(Pb,Zr)TiO_3$, $(Sr,Eu)TiO_3$, $CaTiO_3$, and $BiFeO_3$] listed in Table II. Peculiarities of the bilinear coupling tensors in 32 symmetry classes are listed in Table III.

III. ILLUSTRATION OF SEEMING PARADOX ON TWIN WALLS IN FERROELASTICS

For multiferroics with antiferrodistortive and polar long-range order parameters the conventional forms of the bulk LGD Helmholtz and Gibbs functional densities are $F_b[\mathbf{P},\mathbf{\Phi},\mathbf{u}] = U^u_{\mathrm{LGD}} + U^u_{\mathrm{Elastic}} + U^u_{P\Phi} + U^u_{A\Phi}$ and $G_b[\mathbf{P},\mathbf{\Phi},\boldsymbol{\sigma}] = U^\sigma_{\mathrm{LGD}} + U^\sigma_{\mathrm{Elastic}} + U^\sigma_{P\Phi} + U^\sigma_{A\Phi}$. Typical forms of the LGD contribution $U^{u,\sigma}_{\mathrm{LGD}}$ as a function of the octahedral rotations Φ_i and polarization P_i and elastic contribution $U^{u,\sigma}_{\mathrm{Elastic}}$ that include purely elastic, electrostriction, rotostriction, and flexoelectric coupling terms are listed in Appendix S1 of Supplemental Material in Ref. 53. The flexoantiferrodistortive coupling terms $U^{u,\sigma}_{P\Phi}$ and $U_{A\Phi}$ are given by Eq. (2). Below we will regard $F_b[\mathbf{P},\mathbf{\Phi},\mathbf{u}]$ as Φ-P-u representation and $G_b[\mathbf{P},\mathbf{\Phi},\boldsymbol{\sigma}]$ as Φ-P-σ representation. Starting from the variation of the functional in any of the representations, Euler-Lagrange equations for the polarization and tilt as well as equations of state for the elastic stress or strain can be derived. The equations of state give the relation between the stress and strain. After the substitution of the relation into the Euler-Lagrange equations, an unambiguous relationship between the coefficients of LGD expansion for Φ-P-u representation and Φ-P-σ representation can be established. In particular the biquadratic flexoantiferrodistortive coupling tensor (2a) transforms as $\xi^u_{ijkl} = \xi^\sigma_{ijkl} + f_{ijmn}R_{mnkl}$, and so if one starts from the conventional Φ-P-σ representation with zero ξ^σ_{ijkl}, then it is mandatory to come to nonzero values $\xi^u_{ijkl} = f_{ijmn}R_{mnkl}$ in Φ-P-u representation. In other words the condition $\xi^u_{ijkl} = \xi^\sigma_{ijkl} = 0$ never can be valid and its artificial fulfillment can lead to an unphysical paradox.

For a demonstration of the paradox that appeared when the universal bilinear coupling (2a) *was not included properly* into the LGD potential, we chose ferroelastic $SrTiO_3$, because all its material parameters are relatively well known, including rotostriction,[55–57] and the flexoelectric coupling tensor components were measured experimentally.[58–60] $SrTiO_3$ undergoes the second order phase transition at $T \approx 105$ K from the cubic phase of $m3m$ symmetry to the tetragonal antiferrodistortive phase of $4/mmm$ symmetry with one-component spontaneous tilt Φ_S. Single-domain regions of bulk $SrTiO_3$ are nonpolar, while the flexo-roto coupling can induce a spontaneous polarization in the vicinity of elastic domain walls.[54] Let us consider the typical head-to-head and head-to-tail twin boundaries (TBs) between domains "1" and "2" with different orientation of tilts very far from the wall [see Fig. 1(a)]. Figure 1(b) shows the distribution of the tilts $\tilde{\Phi}_1 \perp$TB and $\tilde{\Phi}_2 \uparrow\uparrow$ TB calculated across head-to-head TB in Φ-P-σ (solid curves) and Φ-P-u (dash-dotted curves) representations without the coupling term (2). The minute difference between the solid and dash-dotted curves originated from the flexoelectric coupling. Polarization components $\tilde{P}_1 \perp$TB and $\tilde{P}_2 \uparrow\uparrow$ TB are induced by the flexocoupling across the TB and vanish far from it for both Φ-P-σ (solid curves) and Φ-P-u (dash-dotted curves) representations, but corresponding curves in Figs. 1(c) and 1(d) look very different. Moreover, $\tilde{P}_2$ is absent in Φ-P-σ representation at temperatures higher than about 36 K, but

TABLE III. Peculiarities of the bilinear coupling tensors in 32 symmetry classes.

Symmetry class		Tensor symbol, structure, and/or nontrivial components (comp.)					
		ζ_{ijk} in Eq. (2a)			ξ_{ijkl} in Eq. (2b)		
		Nonzero comp.	Different comp.	Equal in module but different in sign comp.	Nonzero comp.	Different comp.	Equal in module but different in sign comp.
1	1	27	27	–	81	54	–
2	$\bar{1}$	27	27	–	81	54	–
3	2	13	13	–	41	28	–
4	m	13	13	–	41	28	–
5	$2/m$	13	13	–	41	28	–
6	222	6	6	–	21	15	–
7	$mm2$	6	6	–	21	15	–
8	mmm	6	6	–	21	15	–
9	4	13	10	3	39	20	6
10	$\bar{4}$	13	10	3	39	20	6
11	$\bar{4}2m$	6	6	3	21	9	–
12	422	6	6	3	21	9	–
13	$4/m$	13	10	3	39	20	6
14	$4mm$	6	6	3	21	9	–
15	$4/mmm$	6	6	3	21	9	–
16	3	21	14	5	71	36	11
17	32	10	8	4	38	16	3
18	$3m$	10	8	4	38	16	3
19	$\bar{3}$	21	14	5	71	36	11
20	$\bar{3}m$	6	6	3	38	16	3
21	$\bar{6}$	13	10	3	39	20	6
22	$\bar{6}m2$	6	6	3	21	8	–
23	6	13	10	3	39	20	6
24	622	6	6	3	21	8	–
25	$6/m$	13	10	3	39	20	6
26	$6mm$	6	6	3	21	8	–
27	$6/mmm$	6	6	3	21	8	–
28	23	6	2	–	21	5	–
29	$m3$	6	2	–	21	5	–
30	$\bar{4}3m$	6	2	1	21	3	–
31	432	6	2	1	21	3	–
32	$m3m$	6	2	1	21	3	–

is rather high in Φ-P-u representation [Fig. 1(d)]. Again, the curves for $\tilde{P}_1$ and $\tilde{P}_2$ are calculated *without* the coupling term (2a).

So, one can see the *seeming paradox here*. It is well known that Gibbs and Helmholtz functionals are different, but the values calculated from the Euler-Lagrange equations should be the same. So, what is the physical origin of the difference in polarization profiles calculated in Φ-P-σ and Φ-P-u representations? The additional "roto-flexo" sources of polarization, $\tilde{f}_{66}\tilde{R}_{66}\partial(\tilde{\Phi}_1\tilde{\Phi}_2)/\partial\tilde{x}_1$, appeared in the Euler-Lagrange equations in Φ-P-u representation in contrast to the Φ-P-σ one (see Appendix S2-3 in Ref. 53). By the addition of the coupling (2) the term renormalizes as $(\tilde{\xi}^{\sigma}_{66}+\tilde{f}_{66}\tilde{R}_{66})\partial(\tilde{\Phi}_1\tilde{\Phi}_2)/\partial\tilde{x}_1$ and becomes zero for $\tilde{\xi}^{\sigma}_{66}=-\tilde{f}_{66}\tilde{R}_{66}$. If one starts from the conventional Φ-P-σ representation with zero $\xi^{\sigma}_{ijkl}\equiv 0$, that corresponds to the solid and dotted curves in Figs. 1(c) and 1(d), then it is mandatory that $\xi^{u}_{ijkl}\equiv f_{ijmn}R_{mnkl}$, but not $\xi^{u}_{ijkl}\equiv 0$ as regarded for dashed and dash-dotted curves. These results allow one to regard the value $\xi^{u}_{ijkl}\propto f_{ijmn}R_{mnkl}$ as a reasonable estimation of the flexoantiferrodistortive coupling strength in $SrTiO_3$. This gives $\xi^{u}_{11}\propto -5.08\times 10^{19}$, $\xi^{u}_{12}\propto 2.66\times 10^{19}$, and $\xi^{u}_{11}\propto -1.95\times 10^{19}$ V/m^2.

Beyond the paradox resolution for the $SrTiO_3$ example, we predicted a noticeable influence of the flexoantiferrodistortive coupling on the structure and physical properties of the domain boundaries in the related $Eu_xSr_yBa_{1-x-y}TiO_3$ systems. Significant differences between Φ-P-u and Φ-P-σ curves in Figs. 1(c) and 1(d) give all grounds to expect that the influence can be rather strong and thus it should be mandatory to take flexoantiferrodistortive coupling into account in the future.

IV. MODULATED PHASES CAUSED BY THE FLEXOANTIFERRODISTORTIVE COUPLING

Here we illustrate that the flexoantiferrodistortive coupling strongly influences the order parameters and phase stability regions of multiferroics and leads to the appearance of the incommensurately modulated phases (MPs). In order to derive analytical results, let us consider one-component tilt $\Phi(x)$ and

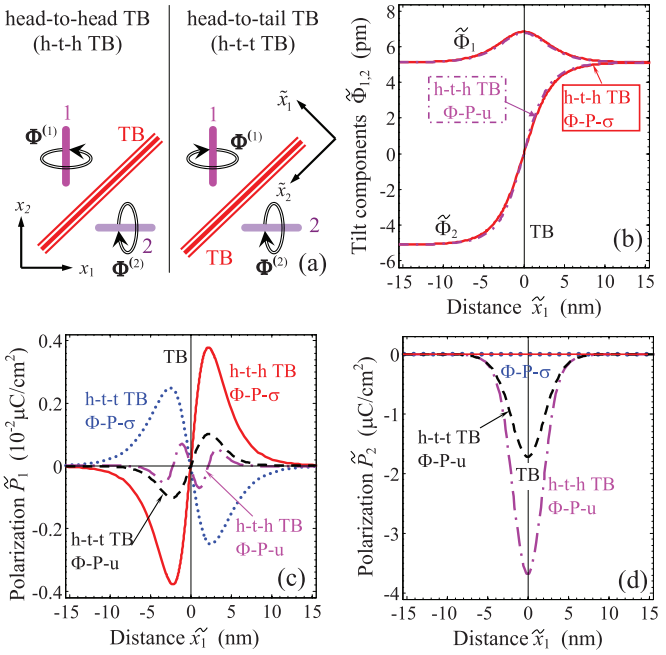

FIG. 1. (Color online) (a) Schematics of head-to-head (h-t-h) and head-to-tail (h-t-t) twins $\mathbf{\Phi}^{(1)} = (\pm\Phi_S,0,0)$ and $\mathbf{\Phi}^{(2)} = (0,\Phi_S,0)$, where the signs "±" correspond to the orientation of the tilt arrows far from the TB. Rotated coordinate system is $\{\tilde{x}_1,\tilde{x}_2\}$. Profiles of tilts $\tilde{\Phi}_1(\tilde{x}_1)$ and $\tilde{\Phi}_2(\tilde{x}_1)$ (b) and polarization components $\tilde{P}_1(\tilde{x}_1)$ (c) and $\tilde{P}_2(\tilde{x}_1)$ (d) across the TB in $SrTiO_3$ at temperature 50 K. Different curves were calculated using Φ-P-σ representation with $\xi^{\sigma}_{ijkl} = 0$ and Φ-P-u representation with $\xi^{u}_{ijkl} = 0$.

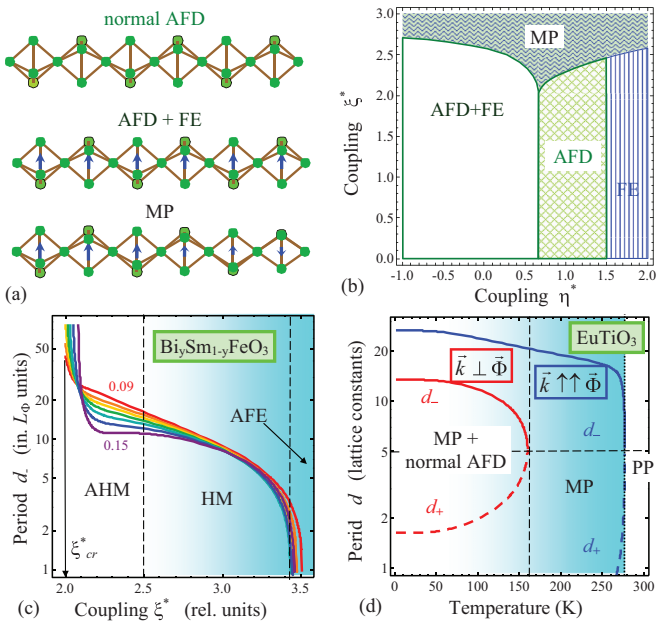

FIG. 2. (Color online) (a) Oxygen octahedrons arrangement in AFD, AFD + FE, and MP phases. Blue arrows indicate the polarization. (b) Phases evolution in dependence on the coupling constants ξ^* and η^* calculated for $\Delta = 0.5$, $g^* = 8$, and $t = -1.5$. (c) IC AFD-modulation period d/L_Φ vs the coupling strength ξ^* calculated for $Bi_ySm_{1-y}FeO_3$ with Sm content $y = 0.09-0.15$ (different curves with y step of 0.01) and $T = 300$ K. AHM indicates the region with anharmonic modulation, HM indicates the harmonic modulation, AFE is the antiferroelectriclike region. (d) Temperature dependence of the IC AFD-modulation periods $d_\pm$ calculated in the MP of $EuTiO_3$ for two modulation directions, $\vec{k}_\pm \uparrow\uparrow \vec{\Phi}$ and $\vec{k}_\pm \perp \vec{\Phi}$. $EuTiO_3$ parameters are listed in the text.

polarization $P_3(x_1) \equiv P(x)$ (one-dimensional theory without depolarization effects). Along with the coupling (2a) LGD potential density acquires the form

$$F_b[P,\Phi] = \beta_1\Phi^2 + \beta_{11}\Phi^4 + \frac{v}{2}\left(\frac{\partial\Phi}{\partial x}\right)^2 + \alpha_1 P^2 + \alpha_{11}P^4 + \frac{g}{2}\left(\frac{\partial P}{\partial x}\right)^2 - \eta P^2\Phi^2 + \frac{\xi}{2}\left[\frac{\partial P}{\partial x}\Phi^2 - P\frac{\partial(\Phi^2)}{\partial x}\right]. \quad (3)$$

Coefficients α_1 and β_1 are linear inverse susceptibilities related to P and tilt Φ; α_{11} and β_{11} are nonlinear generalized stiffness for corresponding order parameter; tilt and polarization gradient coefficients are v and g. The flexoantiferrodistortive coupling coefficient is ξ; η is the biquadratic coupling coefficient. For most of the multiferroics and their solid solutions linear dependences of the coefficients α_1 and β_1 on temperature T are valid; $\alpha_1(T) = \alpha_T(T - T_P)$ and $\beta_1(T) = \beta_T(T - T_\Phi)$, where the polar and antiferrodistortive critical temperatures T_P and T_Φ can be dependent on the chemical composition of multiferroic solid solution. Other coefficients are typically weakly (or at least noncritically) temperature dependent, but can be strongly composition dependent. The energy (3) is stable at high values of order parameters under the conditions $\alpha_{11} > 0$, $\beta_{11} > 0$, $2\sqrt{\alpha_{11}\beta_{11}} - \eta > 0$, $v > 0$, and $g > 0$. Thermodynamically stable phases described by the energy (3), corresponding order parameter values, and stability conditions are listed in Table IV.

Assuming linear temperature dependencies $\alpha_1(T)$ and $\beta_1(T)$ in the functional (3), the system phase diagram depends on the five dimensionless parameters, namely flexoantidistortive and biquadratic coupling constants, $\xi^* = |\xi|/(2\sqrt{v\sqrt{\alpha_{11}\beta_{11}}})$ and $\eta^* = \eta/\sqrt{\alpha_{11}\beta_{11}}$, temperature $(T - T_\Phi)/(T_\Phi - T_P) = t$, and ratios $\Delta = \beta_T\sqrt{\alpha_{11}}/(\alpha_T\sqrt{\beta_{11}})$ and $g^* = g\sqrt{\alpha_{11}}/(v\sqrt{\beta_{11}})$. It appears that the values ξ^* and η^* define the phase diagram. Temperature t should be negative in the ordered phase; its value determines the position of the vertical boundary between AFD + FE, AFD, and FE phases see Table IV. Oxygen octahedrons arrangement in AFD, AFD + FE, and MP phases is schematically shown in Fig. 2(a). Figure 2(b) illustrates the typical evolution of the phases in dependence on the ξ^* and η^*. The MP region is not very sensitive to the values of η^* and t, but requires $|\xi^*|$ values higher than 2. MP strongly enlarges the stability region with the $|\xi^*|$ increase. AFD, AFD + FE, and FE phase boundaries appeared indeed sensitive to the values of η^* and t.

To study analytically the modulation period, which is the most important feature of the MP, we use the harmonic modulation approximations (HMAs) for the order parameter distributions:

$$P = P_0 - \delta P\sin(kx), \quad \Phi = \Phi_0 - \delta\Phi\cos(kx). \quad (4a)$$

TABLE IV. Thermodynamically stable bulk phases of the free energy [Eq. (3)].

Phase description and abbreviation	Order parameters	Stability condition
Parent (PP)	$P = \Phi = 0$	$\alpha_1 > 0,\ \beta_1 > 0$
Antiferrodistortive (normal AFD)	$\Phi = \pm\sqrt{-\beta_1/2\beta_{11}},\ P = 0$	$\beta_1 < 0,\ 2\alpha_1 + \eta(\beta_1/\beta_{11}) > 0$
Antiferrodistortive-ferroelectric (normal AFD + FE)	$\Phi = \sqrt{-\frac{2\beta_1+\eta(\alpha_1/\alpha_{11})}{4\beta_{11}-(\eta^2/\alpha_{11})}}$,	$2\alpha_1 + \eta(\beta_1/\beta_{11}) < 0,$,
	$P = \sqrt{-\frac{2\alpha_1+\eta(\beta_1/\beta_{11})}{4\alpha_{11}-(\eta^2/\beta_{11})}}$	$2\beta_1 + \eta(\alpha_1/\alpha_{11}) < 0,\ 2\sqrt{\alpha_{11}\beta_{11}} > -\eta,$
Ferroelectric (FE)	$P = \sqrt{-\alpha_1/2\alpha_{11}},\ \Phi = 0$	$\alpha_1 < 0,\ 2\beta_1 + \eta(\alpha_1/\alpha_{11}) > 0$
Incommensurate AFD modulated	In harmonic approximation	$\xi^2 \geqslant \beta_{11}\left[\sqrt{2g} + \sqrt{-\frac{v}{2\beta_1}\left(2\alpha_1 + \eta\frac{\beta_1}{\beta_{11}}\right)}\right]^2,$
phase (MP) with possible AFE phase	$P = P_0 - \delta P\sin(kx),$ $\Phi = \Phi_0 - \delta\Phi\cos(kx)$	$2\alpha_1 + \eta(\beta_1/\beta_{11}) > 0,\ \beta_1 < 0$

HMA is valid in the vicinity of the MP boundaries. The modulation number k, "base" Φ_0 and P_0, and amplitudes δP and $\delta\Phi$ are variational parameters determined from the energy (3) minimization (see Appendix S4 in Ref. 53). The relationship between k and ξ is

$$\frac{vg}{4k^2\Phi_0^2}\left(k^2 + \frac{1}{L_\Phi^2}\right)\left(k^2 + \frac{1}{L_P^2}\right) = \xi^2. \tag{4b}$$

The solution of biquadratic Eq. (4b) for the modulation vector is $k_\pm = \sqrt{(-b \pm \sqrt{b^2 - 4c})/2}$, where $b = L_P^{-2} + L_\Phi^{-2} - 4\xi^2\Phi_0^2/(vg)$ and $c = L_P^{-2}L_\Phi^{-2}$. Here we introduced the polar and structural correlation lengths as $L_P = \sqrt{g[2\alpha_1 + \eta(\beta_1/\beta_{11})]^{-1}}$ and $L_\Phi = \sqrt{v/(-4\beta_1)}$ correspondingly, which are positive in the AFD MP. Using that $|\Phi_0| \gg |\delta\Phi|$, $\Phi_0 \approx \pm\sqrt{-\beta_1/2\beta_{11}}$, $P_0 = 0$, and δP is small in the vicinity of MP-AFD boundary, approximate expressions for the MP-AFD phase boundary and the wave vector at the boundary k_b were derived:

$$\xi^2 = \frac{gv}{4\Phi_0^2}\left(\frac{1}{L_P} + \frac{1}{L_\Phi}\right)^2, \quad k_b = \sqrt{\frac{1}{L_P L_\Phi}}. \tag{5}$$

In fact Eq. (5) determines the minimal critical value of the coupling strength, ξ_{cr}, required for the commensurate-incommensurate phase transition. The physical sense of the condition $|\xi| \geqslant \xi_{cr}$ is that the effective length induced by the flexoantiferrodistortive coupling should be higher than the sum of inverse polar and structural correlation lengths, since exactly $\xi_{cr}^2 \propto (L_P^{-1} + L_\Phi^{-1})^2$ per Eq. (5). The modulation profile is quasiharmonic if the half period π/k is not much higher than the effective correlation length, $L_C = L_P L_\Phi/(L_P + L_\Phi)$. Though the main results (2)–(5), Tables II–IV, and phase evolution shown in Fig. 2(b) are *universal* (i.e., not material specific), let us consider briefly their applications for the determination of the ICP modulation period in concrete materials.

ICP was observed in antiferrodistortive multiferroic $Bi_ySm_{1-y}FeO_3$ for Sm content $y \propto 0.1$ at room temperature.[24] Using Eqs. (3)–(4b) for $Bi_ySm_{1-y}FeO_3$ parameters, namely the transition temperature from cubic phase into the orthorhombic one, $T_\Phi(y) = T_{\Phi 0} + (T_{\Phi 1} - T_{\Phi 0})y$, $T_{\Phi 0} =$ 1200 K, and $T_{\Phi 1} = 1100$ K,[61] ferroelectric Curie temperature $T_P(y) = T_{P0}[1 - (y/y_{cr})]^{1/2}$, $T_{P0} = 1120$ K, and $y_{cr} = 0.16$,[62] we calculated the dependence of the modulation period $d_\pm = 2\pi/k_\pm$ on the flexoantiferrodistortive coupling value ξ^*. Figure 2(c) illustrates that the ICP modulation period d_-/L_Φ diverges at $\xi^* \to \xi_{cr}^*$, then rapidly decreases with ξ^* increase, and becomes zero at $\xi^* \approx 3.5$. When the period becomes compatible or smaller than the lattice constant, it indicates the origin of antiferroelectriclike (AFE) polarization. Since typically L_C is about a lattice constant, the inequality $d \leqslant L_C$ determines the AFE phase transition that appeared at $\xi^* \geqslant 3.4$ in agreement with experiment.[24]

Goian *et al.*[25] observed the incommensurate AFD tetragonal structure in $EuTiO_3$ with periodicity of about 16 unit cells below 300 K. Kim and Ryan[26] reported about the incommensurate AFD-AFE superstructure periodicity of about 14 unit cells below 285 K in $EuTiO_3$. Using Eqs. (3)–(4b) for $EuTiO_3$, we assume that coefficient $\alpha_1(T)$ depends on temperature T in accordance with the Barrett law,[63] $\alpha_1(T) = \alpha_T^{(P)}T_q^{(P)}[\coth(T_q^{(P)}/T) - \coth(T_q^{(P)}/T_c^{(P)})]$. Coefficient $\alpha_T^{(P)} = 0.98 \times 10^6$ m/(F K), $T_q^{(P)} \approx 115$ K is the called quantum vibration temperature, and $T_c^{(P)} \approx -133$ K is the "effective" Curie temperature corresponding to the polar soft mode in bulk $EuTiO_3$.[64,65] To account for the experiment and Barrett law the coefficient $\beta_1(T)$ depends on temperature as $\beta_1(T) = \beta_T^{(\Phi)}T_q^{(\Phi)}[\coth(T_q^{(\Phi)}/T) - \coth(T_q^{(\Phi)}/T_c^{(\Phi)})]$, where $\beta_T^{(\Phi)} = 1.96 \times 10^{26}$ J/(m^5 K), $T_q^{(\Phi)} \approx 102$ K, $T_c^{(\Phi)} \approx 281$ K.[66,67] In particular this gives that $\beta_1 = -3.75 \times 10^{28}$ J/m^5 and $\alpha_1 = 2.73 \times 10^8$ m/F at $T = 5.2$ K. Parameters $\beta_{11} = 0.436 \times 10^{50}$ J/m^7, $v_{11} = 0.28 \times 10^{10}$ J/m^3, $v_{44} = 7.34 \times 10^{10}$ J/m^3, $\alpha_{11} = 1.6 \times 10^9$ m^5/(C^2 F), $g \approx 0.3 \times 10^{-10}$ V m^3/C, $\eta_{11} = 2.23 \times 10^{29}$ (F m)$^{-1}$, $\eta_{12} = -0.85 \times 10^{29}$ (F m)$^{-1}$ (Ref. 53) and modulation period $d \cong (10{-}20)$ lattice constants (*l.c.*) we estimated the coupling constant ξ. Depending on the tilt orientation $\vec{\Phi}$ with respect to the direction of modulation vector $\vec{k} \uparrow\uparrow x$ we obtained that $\xi = \xi_{11} = 3 \times 10^{20}$ V/m^2 for the case $\vec{k} \uparrow\uparrow \vec{\Phi}$ when $v = v_{11}$ and $\eta = \eta_{11}$; meanwhile $\xi = \xi_{12} = 2.6 \times 10^{20}$ V/m^2 for the case $\vec{k} \perp \vec{\Phi}$, when $v = v_{44}$ and $\eta = \eta_{12}$. Shown in Fig. 2(d) ICP modulation periods $d_\pm = 2\pi/k_\pm$ are in the range 2–20 *l.c.* depending on temperature and $\vec{\Phi}$ orientation. When the period d_+ becomes compatible or smaller than 2 *l.c.* for $\vec{k}_+ \uparrow\uparrow \vec{\Phi}$ and temperatures lower than 110 K, it may indicate the origin of coexisting AFE polarization.

Emergence of spatially modulated polarization and tilt at the structural domain walls of $EuTiO_3$ are shown in Fig. 3. The modulation is absent without the flexoantiferrodistortive

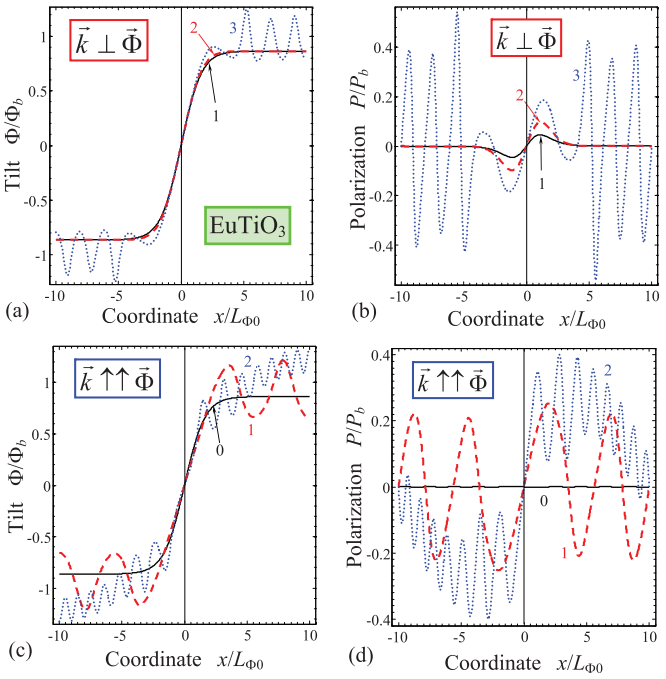

FIG. 3. (Color online) Tilt (a), (c) and polarization (b), (d) spatial modulation originated near $EuTiO_3$ antiphase boundary between the domains with opposite orientations of tilt vector calculated for different values of flexoantiferrodistortive coupling coefficient. For orientation $\vec{k}\perp\vec{\Phi}$ (a), (b) the value $\xi = \xi_{12} = 1$, 2, and 3×10^{20} V/m^2 (solid, dashed, and dotted curves, respectively). For orientation $\vec{k} \uparrow\uparrow \vec{\Phi}$ (c), (d) the value $\xi = \xi_{11} = 0$, 1, and 2×10^{20} V/m^2 (solid, dashed, and dotted curves, respectively). Temperature $T = 200$ K; scales for the tilt, polarization, and x coordinate are introduced as $\Phi_b = \sqrt{\beta_T^{(\Phi)} T_q^{(\Phi)}/(2\beta_{11})}$, $P_b = \sqrt{\beta_T^{(\Phi)} T_q^{(\Phi)}/2\sqrt{\beta_{11}\alpha_{11}}}$, and $L_{\Phi 0} = \sqrt{v/(2\beta_T^{(\Phi)} T_q^{(\Phi)})}$, where $v = v_{11}$ for $\vec{k} \uparrow\uparrow \vec{\Phi}$ and $v = v_{44}$ for $\vec{k}\perp\vec{\Phi}$. $EuTiO_3$ parameters are listed in the text.

coupling as well as when the coupling strength is smaller that the critical value (see solid curves). It originates for the coupling strength higher then the critical value dependent on the modulation vector $\vec{k}$ orientation with respect to the tilt $\vec{\Phi}$ (compare dashed curves for $\vec{k} \uparrow\uparrow \vec{\Phi}$ and $\vec{k}\perp\vec{\Phi}$). Finally the polarization modulation amplitude increases and its period decreases with the coupling value increase (see dotted curves which look completely incommensurate). Note, that in agreement with experimental observations[26] the spatial modulation of polarization can acquire antiferroelectric features for the case $\vec{k}\perp\vec{\Phi}$ and high values of $\xi = 3\times10^{20}$ V/m^2 [see dotted curves in Fig. 3(b)].

V. SUMMARY

Our analysis provides new insight into origins of morphotropic and nanoscale phase-separated systems in complex oxide multiferroics that have eluded macroscopic description. Namely, we show that a universal flexoantiferrodistortive coupling between the (anti)polarization gradient and the structural long-range order parameter should be included in the LGD functional of antiferrodistortive materials. The coupling tensor components should be either calculated from the first principles or determined experimentally. Using the classical example of antiferrodistortive incipient ferroelectric $SrTiO_3$ we estimated the coupling strength as the convolution of the flexoelectric and rotostriction coupling tensors.

The coupling strongly influences the physical properties and phase diagrams of the multiferroic with ferroelectric and antiferrodistortive phases, primarily leading to the appearance of the spatially modulated mixed phases. Incommensurate modulation appears spontaneously when the coupling strength exceeds the critical value proportional to the sum of inverse polar and structural correlation lengths (commensurate-incommensurate phase transition). We demonstrated that the modulated phase appears and strongly enlarges its stability region with the coupling strength increase. Further increase of the coupling strength can lead to the modulated antiferroelectriclike antiferrodistortive phase. The scenario seems principally different from the known ones[47–52].

Concrete examples of the proposed scenario applicability to real systems, where the incommensurate modulation was observed, are multiferroics solid solution $Bi_ySm_{1-y}FeO_3$[24] and single-phase $EuTiO_3$.[25,26] Also the proposed description could be helpful in the design of the ferroics with advanced properties. A promising candidate could be a $Eu_xSr_yBa_{1-x-y}TiO_3$ solid solution,[68] recently used as a successful alternative to $Eu_xBa_{1-x}TiO_3$ ceramics for searching for the fundamental electric dipole moment of the electron.[69–71] Our approach establishes the ranges of possible phases as a function of composition and temperature and thus can help to design magnetoelectric $Eu_xSr_yBa_{1-x-y}TiO_3$ solid solutions, which have a purely ferroelectric phase without incommensurate antiferrodistortive and/or modulated phases.

ACKNOWLEDGMENTS

The work was supported in part (S.V.K., A.B.) by the U.S. Department of Energy, Basic Energy Sciences, Materials Sciences and Engineering Division, the National Science Foundation Grants No. DMR-1210588 and No. DMR-0820404 (V.G., L.Q.C., and Y.G.). A.N.M. and E.A.E. acknowledge Prof. Yulian M. Vysochanskii for fruitful discussion as well as the State Fund of Fundamental State Fund of Fundamental Research of Ukraine, SFFR-NSF Project No. UU48/002 (NSF Grant No. DMR-1210588).

*sergei2@ornl.gov
†morozo@i.com.ua

[1] N. A. Spaldin and M. Fiebig, Science **309**, 391 (2005).
[2] J. M. Rondinelli and N. A. Spaldin, Adv. Mater. **23**, 3363 (2011).
[3] M. Fiebig, T. Lottermoser, D. Frohlich, A. V. Goltsev, and R. V. Pisarev, Nature **419**, 818 (2002).

[4]R. Ramesh and N. A. Spaldin, Nat. Mater. **6**, 21 (2007).
[5]M. Fiebig, J. Phys. D: Appl. Phys. **38**, R123 (2005).
[6]P. J. Ryan, J.-W. Kim, T. Birol, P. Thompson, J.-H. Lee, X. Ke, P. S. Normile, E. Karapetrova, P. Schiffer, S. D. Brown, C. J. Fennie, and D. G. Schlom, Nat. Commun. **4**, 1334 (2013).
[7]M. J. Haun, E. Furman, T. R. Halemane, and L. E. Cross, Ferroelectrics **99**, 55 (1989).
[8]B. Houchmanzadeh, J. Lajzerowicz, and E. Salje, J. Phys.: Condens. Matter **3**, 5163 (1991).
[9]E. V. Balashova and A. K. Tagantsev, Phys. Rev. B **48**, 9979 (1993).
[10]A. K. Tagantsev, E. Courtens, and L. Arzel, Phys. Rev. B **64**, 224107 (2001).
[11]M. Daraktchiev, G. Catalan, and J. F. Scott, Phys. Rev. B **81**, 224118 (2010).
[12]O. Dieguez, P. Aguado-Puente, J. Junquera, and J. Iniguez, Phys. Rev. B **87**, 024102 (2013).
[13]M. Imada, A. Fujimori, and Y. Tokura, Rev. Mod. Phys. **70**, 1039 (1998).
[14]E. Dagotto, Science **309**, 257 (2005).
[15]K. H. Ahn, T. Lookman, and A. R. Bishop, Nature **428**, 401 (2004).
[16]A. A. Bokov and Z. G. Ye, J. Mater. Sci. **41**, 31 (2006).
[17]Z. Kutnjak, J. Pelzelt, and R. Blinc, Nature **441**, 956 (2006).
[18]D. I. Woodward, J. Knudsen, and I. M. Reaney, Phys. Rev. B **72**, 104110 (2005).
[19]B. Noheda, Curr. Opin. Solid State Mater. Sci. **6**, 27 (2002).
[20]C. J. Cheng, D. Kan, S. H. Lim, W. R. McKenzie, P. R. Munroe, L. G. Salamanca-Riba, R. L. Withers, I. Takeuchi, and V. Nagarajan, Phys. Rev. B **80**, 014109 (2009).
[21]V. Wadhawan, *Introduction to Ferroic Materials* (CRC Press, Boca Raton, FL, 2000).
[22]A. Khachaturyan and D. Viehland, Mater. Trans. A **38**, 2308 (2007); **38**, 2317 (2007).
[23]R. Pirc, R. Blinc, and J. F. Scott, Phys. Rev. B **79**, 214114 (2009).
[24]A. Y. Borisevich, E. A. Eliseev, A. N. Morozovska, C.-J. Cheng, J.-Y. Lin, Y. H. Chu, D. Kan, I. Takeuchi, V. Nagarajan, and S. V. Kalinin, Nat. Commun. **3**, 775 (2012).
[25]V. Goian, S. Kamba, O. Pacherová, J. Drahokoupil, L. Palatinus, M. Dušek, J. Rohlíček, M. Savinov, F. Laufek, W. Schranz, A. Fuith, M. Kachlík, K. Maca, A. Shkabko, L. Sagarna, A. Weidenkaff, and A. A. Belik, Phys. Rev. B **86**, 054112 (2012).
[26]J.-W. Kim, P. Thompson, S. Brown, P. S. Normile, J. A. Schlueter, A. Shkabko, A. Weidenkaff, and P. J. Ryan, Phys. Rev. Lett. **110**, 027201 (2013).
[27]Y. M. Jin, Y. U. Wang, A. G. Khachaturyan, J. F. Li, and D. Viehland, J. Appl. Phys. **94**, 3629 (2003).
[28]Y. M. Jin, Y. U. Wang, A. G. Khachaturyan, J. F. Li, and D. Viehland, Phys. Rev. Lett. **91**, 197601 (2003).
[29]Y. U. Wang, Phys. Rev. B **73**, 014113 (2006).
[30]S. Kaufmann, U. K. Rößler, O. Heczko, M. Wuttig, J. Buschbeck, L. Schultz, and S. Fähler, Phys. Rev. Lett. **104**, 145702 (2010).
[31]Sh. M. Kogan, Sov. Phys. Solid State **5**, 2069 (1964).
[32]A. K. Tagantsev, Phys. Rev B **34**, 5883 (1986).
[33]V. G. Bar'yakhtar, V. A. L'vov, and D. A. Yablonskii, JETP Lett. **37**, 673 (1983).
[34]M. Mostovoy, Phys. Rev. Lett. **96**, 067601 (2006).
[35]A. Sparavigna, A. Strigazzi, and A. Zvezdin, Phys. Rev. B **50**, 2953 (1994).
[36]A. P. Pyatakov and A. K. Zvezdin, Eur. Phys. J. B **71**, 419 (2009).
[37]B. M. Tanygin, J. Magn. Magn. Mater. **323**, 616 (2011).
[38]T. A. Aslanyan and A. P. Levanyuk, Fiz. Tverd. Tela (Leningrad) **20**, 3336 (1978).
[39]A. L. Korzhenevskii, Zh. Eksp. Teor. Fiz. **81**, 1071 (1981).
[40]V. Gopalan and D. B. Litvin, Nat. Mater. **10**, 376 (2011).
[41]M. S. Majdoub, P. Sharma, and T. Cagin, Phys. Rev. B **77**, 125424 (2008).
[42]S. V. Kalinin and V. Meunier, Phys. Rev B **77**, 033403 (2008).
[43]R. Maranganti and P. Sharma, Phys. Rev. B **80**, 054109 (2009).
[44]E. A. Eliseev, A. N. Morozovska, M. D. Glinchuk, and R. Blinc, Phys. Rev. B. **79**, 165433 (2009).
[45]P. Zubko, G. Catalan, and A. K. Tagantsev, Annu. Rev. Mater Res. **43**, 387 (2013).
[46]H. He and X. Tan, Phys. Rev. B **72**, 024102 (2005).
[47]A. P. Levanyuk, S. A. Minyukov, and A. Cano, Phys. Rev. B **66**, 014111 (2002).
[48]S. V. Berezovsky, V. Yu. Korda, and V. F. Klepikov, Phys. Rev. B **64**, 064103 (2001).
[49]K. Z. Rushchanskii, Y. M. Vysochanskii, and D. Strauch, Phys. Rev. Lett. **99**, 207601 (2007).
[50]A. N. Morozovska, E. A. Eliseev, J. J. Wang, G. S. Svechnikov, Y. M. Vysochanskii, V. Gopalan, and L. Q. Chen, Phys. Rev. B **81**, 195437 (2010).
[51]T. A. Aslanian and A. P. Levanyuk, Pis'ma Zh. Eksp. Teor. Fiz. **28**, 76 (1978).
[52]J. L. Ribeiro and L. G. Vieira, Phys. Rev. B **82**, 064410 (2010).
[53]See Supplemental Material at http://link.aps.org/supplemental/10.1103/PhysRevB.88.224105 for details of calculations.
[54]A. N. Morozovska, E. A. Eliseev, M. D. Glinchuk, L. -Q. Chen, and V. Gopalan, Phys. Rev. B **85**, 094107 (2012).
[55]W. Cao and G. R. Barsch, Phys. Rev. B **41**, 4334 (1990).
[56]P. A. Fleury, J. F. Scott, and J. M. Worlock, Phys. Rev. Lett. **21**, 16 (1968).
[57]N. A. Pertsev, A. K. Tagantsev, and N. Setter, Phys. Rev. B **61**, R825 (2000).
[58]P. Zubko, G. Catalan, P. R. L. Welche, A. Buckley, and J. F. Scott, Phys. Rev. Lett. **99**, 167601 (2007).
[59]P. Zubko, G. Catalan, P. R. L. Welche, A. Buckley, and J. F. Scott, Phys. Rev. Lett. **100**, 199906(E) (2008).
[60]Also we would like to add that we did not know any other measurements of the flexoelectric coupling in $SrTiO_3$. Moreover the values estimated from the ones of Zubko *et al.* (Ref. 59) ($F_{11} = -1.38$, $F_{12} = 0.66$, $F_{44} = 0.848\ 10^{-11}\ C^{-1}\ m^3$) are in reasonable agreement with microscopic theoretical estimations made by Kogan (Ref. 31) very long ago ($f \sim 4$ V and so $F \sim 10^{-11}\ C^{-1}\ m^3$), as well as with the values $F_{11} = 2.46$, $F_{12} = 0.48$, $F_{44} = 0.05$ in $10^{-11}\ C^{-1}\ m^3$ coming from recent theoretical *ab initio* calculations for $(Ba_{1/2}Sr_{1/2})TiO_3$ [I. Ponomareva, A. K. Tagantsev, and L. Bellaiche, Phys. Rev. B **85**, 104101 (2012)]. The values are indeed much smaller than the ones $\sim(5–10) \times 10^{-10}\ C^{-1}\ m^3$ measured by Ma and Cross [W. Ma and L. E. Cross, Appl. Phys. Lett. **82**, 3293 (2003)] for Pb(Zr, Ti)O_3.
[61]G. Catalan and J. F. Scott, Adv. Mater. **21**, 2463 (2009).
[62]V. V. Lemanov, Fiz. Tverd. Tela **39**, 1468 (1997).
[63]J. H. Barrett, Phys. Rev. **86**, 118 (1952).
[64]T. Katsufuji and H. Takagi, Phys. Rev. B **64**, 054415 (2001).
[65]V. Goian, S. Kamba, J. Hlinka, P. Vanek, A. A. Belik, T. Kolodiazhnyi, and J. Petzelt. Eur. Phys. J. B **71**, 429 (2009).

[66] A. Bussmann-Holder, J. Köhler, R. K. Kremer, and J. M. Law, Phys. Rev. B **83**, 212102 (2011).

[67] A. P. Petrović, Y. Kato, S. S. Sunku, T. Ito, P. Sengupta, L. Spalek, M. Shimuta, T. Katsufuji, C. D. Batista, S. S. Saxena, and C. Panagopoulos, Phys. Rev. B **87**, 064103 (2013).

[68] V. Goian, S. Kamba, P. Vaněk, M. Savinov, C. Kadlec, and J. Prokleška, Phase Transitions **86**, 191 (2013).

[69] K. Z. Rushchanskii, S. Kamba, V. Goian, P. Vaněk, M. Savinov, J. Prokleška, D. Nuzhnyy, K. Knížek, F. Laufek, S. Eckel, S. K. Lamoreaux, A. O. Sushkov, M. Ležaic, and N. A. Spaldin, Nat. Mater. **9**, 649 (2010).

[70] A. O. Sushkov, S. Eckel, and S. K. Lamoreaux, Phys. Rev. A **81**, 022104 (2010).

[71] S. Eckel, A. O. Sushkov, and S. K. Lamoreaux, Phys. Rev. Lett. **109**, 193003 (2012).